Available online at www.sciencedirect.com

ScienceDirect

Mendeleev Commun., 2018, **28**, 167–169

Mendeleev Communications

Microwave-assisted synthesis of ultra-small iron oxide nanoparticles for biomedicine

Tatiana A. Lastovina,*[a] Andriy P. Budnyk,[a] Stanislav P. Kubrin[b] and Alexander V. Soldatov[a]

[a] *International Research Center 'Smart Materials', Southern Federal University, 344090 Rostov-on-Don, Russian Federation. E-mail: lastovina@sfedu.ru*

[b] *Department of Physics, Southern Federal University, 344090 Rostov-on-Don, Russian Federation*

DOI: 10.1016/j.mencom.2018.03.019

An efficient method of microwave-assisted synthesis of Sm^{3+}-doped γ-Fe_2O_3 nanoparticles of about 4.5 nm for magnetic imaging in biomedicine is proposed.

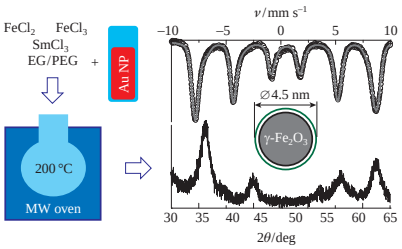

Iron oxide nanoparticles (NPs) possess unique magnetic properties making them attractive for biomedical applications.[1] NPs are expected to be small enough to remain in blood circulation after injection, to be capable of passing through the capillary system of organs and tissues, to be coated with hydrophilic molecules preventing agglomeration and avoiding plasma protein adsorption.[2] For that use NPs are most commonly prepared in magnetite (Fe_3O_4) and maghemite (γ-Fe_2O_3) phases.[3] In order to tune their magnetic response, iron oxides can be further doped with rare-earth metal ions like Sm^{3+}, Eu^{3+} and Gd^{3+}.[4]

Coprecipitation is a conventional method for the production of magnetic NPs.[5,6] Microwave (MW) heating used for the synthesis increases the rate of reaction with preserving a good control over the formation of particles.[7] Note that the coprecipitation of tiny amounts of noble metals[8(a)] or deposition onto the surface of noble metals[8(b)] can mitigate nucleation of non-nobles, resulting in a decrease of NP size. For instance, gold NPs alone or in combination with iron oxides are widely utilized in biomedicine to form nanocomposites.[8(c)]

We used the modified coprecipitation of $FeCl_2$ and $FeCl_3$ salts in aqueous solution to produce γ-Fe_2O_3 NPs of 11–13 nm doped by Sm^{3+}, Eu^{3+} and Gd^{3+} ions.[9(a)] Alternatively, a solvothermal polyol method allowed us to obtain the Sm^{3+}-doped Fe_3O_4 NPs of 9–23 nm from $FeCl_3$ and $SmCl_3$ precursors.[9(b)] MW heating of $Fe(acac)_3$ in pure oleylamine or in its mixture with oleic acid resulted in γ-Fe_2O_3 NPs of 5 nm.[9(c)] Here, we report on the ultra-small Sm^{3+}-doped iron oxide NPs obtained by a MW-assisted one-pot polyol coprecipitation synthesis in the presence of gold NPs.†

The XRD patterns‡ of the synthesized S0 and S1 samples are presented in Figure 1(*a*). The profile of S1 [Figure 1(*a*), black] contains the reflections indexed into a cubic spinel structure.[10] The calculated lattice parameter and crystallite size are 8.369(2) Å and 4 nm, respectively (see Online Supplementary Materials for details). The absence of any other reflections suggests that (i) Sm^{3+}

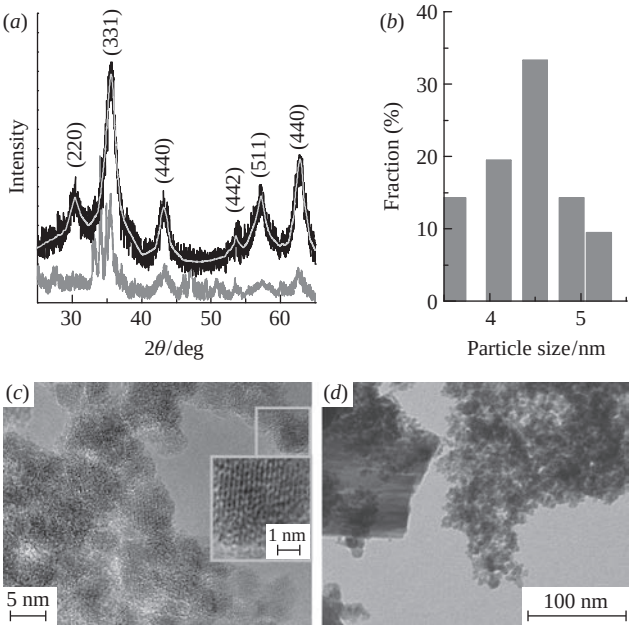

Figure 1 Structural characterization of synthesized iron oxide NPs: (*a*) XRD patterns of S0 (grey) and S1 (black) samples, (*b*) particle size distribution histogram for S1 sample, (*c*) TEM image for S1 with magnification of a particle and (*d*) TEM image for S0 sample.

† Commercial reagents were used as received. In a typical synthesis, $FeCl_2$ (0.2 mmol), $FeCl_3$ (0.4 mmol) and $SmCl_3$ (9 μmol) were dissolved in EG/PEG (10/1 ml) solution. Then, NaOH (3 mmol) in EG (2.4 ml) and 3.65 ml of a commercial gold NP solution (5 nm in diameter, 5.5×10^{13} NPs ml^{-1}) were added. The mixture was heated in a MW reactor (Discover SP, CEM, USA) for 3 h at 473 K. After cooling to room temperature, the black precipitate was washed several times with ethanol and deionized water and collected with a permanent magnet. The obtained powder was dried overnight in a vacuum oven at 333 K. This sample will be referred as S1. A blank sample, S0, without addition of gold NPs was also produced.

‡ X-ray diffraction (XRD) pattern was recorded on ARL X'TRA; X-ray fluorescence (XRF) analysis was performed on M4 Tornado Micro-XRF; transmission electron microscopy (TEM) images were acquired at Titan 80-300; the Mössbauer spectra were measured on MS-1104Em; IR spectrum was collected on FSM-2012; UV-VIS spectrum was recorded on UV-2600; magnetization curve was obtained on VSM7400.

can be incorporated into the crystalline lattice occupying Fe^{3+} sites[11] and (ii) the amount of remaining gold NPs appears below the detection limit of the instrument. The actual quantities of samarium and gold in S1 were evaluated by Micro-XRF analysis,‡ which gave the concentrations of Sm and Au (in respect to Fe) of 2.95 and 0.95 wt%, respectively. The diffraction pattern for S0 expresses less distinct features due to impure phase (co-presence of α-Fe_2O_3).

In harmony with XRD data, TEM imaging‡ confirms the formation of ultra-small NPs as evidenced by a particle size distribution histogram [Figure 1(*b*),(*c*)]. The particles appear round-like [see Figure 1(*c*)], their average size of ~4.5 nm matches well with that found from XRD, indicating the single crystal nature of obtained NPs. The size coincides with that of introduced gold NPs (5 nm), evidencing a size equivalence of the composite components. A TEM image for S0 sample [Figure 1(*d*)] contains both ultra-small round NPs of a spinel phase and right-shaped micro-sized pieces of α-Fe_2O_3 phase, in correspondence to its XRD pattern [Figure 1(*a*), grey].

We employed Mössbauer spectroscopy‡ for phase identification and characterization of iron state. The Mössbauer spectrum acquired at 300 K is shown in Figure 2. It consists of a superparamagnetic doublet, which is typical of maghemite NPs.[12(*a*)] The doublet exhibits an isomer shift of ~0.35 mm s^{-1} and a quadrupole split of ~0.7 mm s^{-1}, evidencing for the Fe^{3+} state.[12(*b*)] The spectrum collected at 13 K (Figure 2) exhibits a magnetic splitting into three sextets (Table S1, see Online Supplementary Materials). The sextet S#1 (according to its isomer shift) corresponds to a Fe^{3+} octahedron oxygen environment,[12(*b*)] while the sextet S#2 refers to Fe^{2+} in a tetrahedron oxygen environment. Both S#1 and S#2 sextets are a common feature of the γ-Fe_2O_3 NPs spectra measured at extremely low temperatures.[12(*a*)] However, there is another sextet S#3. It also exhibits Fe^{3+} state but has the lowest value of hyperfine magnetic field. This allows us to suggest that the sextet S#3 may relate to surface ions of NPs. Hence,

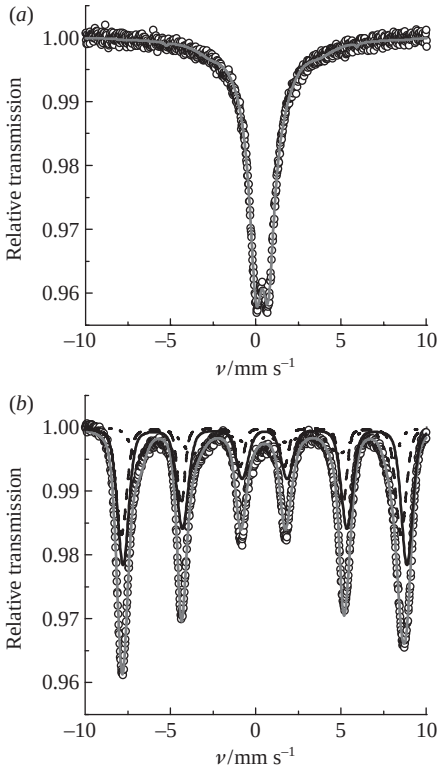

Figure 2 Mössbauer spectra of iron oxide NPs measured at (*a*) 300 and (*b*) 13 K. Experimental data are shown with circles together with fitting curves (dark grey). Spectrum at 13 K is also deconvoluted into three sextets S#1 (solid line), S#2 (dashed) and S#3 (dotted).

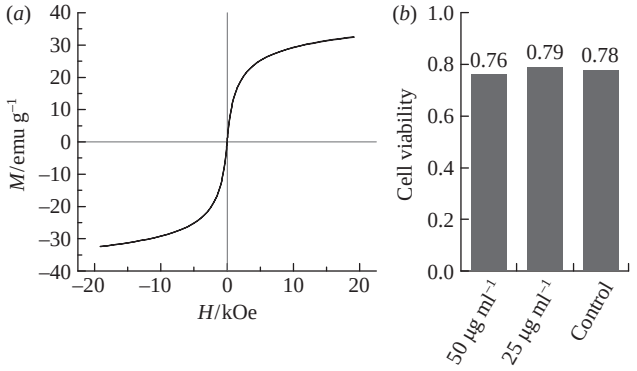

Figure 3 (*a*) Magnetization curve and (*b*) the results of a viability test on HeLa cells where solutions with concentrations of 50 and 25 μg ml^{-1} were used.

these results undoubtedly confirm the formation of γ-Fe_2O_3 phase possessing magnetic properties.

The results of UV-VIS and IR spectroscopies (details are given in Online Supplementary Materials) allowed us to conclude that small maghemite NPs are covered with polyol shells attached to particle surface *via* carboxylic groups. The measured *M–H* curve [Figure 3(*a*)] has no hysteresis loop and coinciding branches with saturation magnetization of about 33 emu g^{-1}. Such a profile clearly indicates a superparamagnetic behavior, which characterizes the obtained material as ultra-small superparamagnetic iron oxide NPs, so-called SPIONs. Scarcely distributed gold NPs and thin covering layer over iron oxide NPs are beneficial factors for MRI because the formation of a dense gold shell around NPs may weaken their response to an external magnetic field.[13]

The biocompatibility test was performed as a standard evaluation of acute toxicity towards HeLa cells using live/dead assays (for details, see Online Supplementary Materials). The formulations of NPs were resuspended in physiological saline to reach 50 and 25 μg ml^{-1} concentrations of final culture medium. The values of averaged viability proportion were 0.79 and 0.76, respectively [Figure 3(*b*), Table S2]. It is clear that the viability of cells after contacting with a 25 μg ml^{-1} solution remains similar to that in control physiological solution (without NPs). A double increase of concentration (50 μg ml^{-1}) has a minimal cytotoxic effect. These results are encouraging and correspond to the literature data.[14]

In conclusion, SPIONs with Sm^{3+} doping of 2.95 wt% (XRF) were prepared just in a few hours by a novel MW-assisted coprecipitation route with the addition of a small quantity of gold NPs. Such a level of Sm^{3+} doping meets the requirements for a contrast agent for MRI. The presence of gold NPs appears to be essential in assisting the complete conversion of metal precursors into NPs. Prepared NPs are of γ-Fe_2O_3 phase (XRD and Mössbauer) with average size of ~4.5 nm (TEM and XRD). This size is two or three times smaller than that of NPs produced by coprecipitation polyol syntheses in conventional reactors (three-neck flasks or autoclaves).[9(*a*),(*b*)] SPIONs are covered by a thin layer of partially oxidized glycol molecules (FTIR). Prepared materials showed low toxicity towards HeLa cells (0.76–0.79).

This study was supported by the Russian Science Foundation (project no. 14-35-00051). We are grateful to Dr. P. Zolotukhin and A. Belanova (Evolution corporate group) for their assistance in performing the cytotoxicity test, and to National Research Centre ‘Kurchatov Institute’ for TEM imaging.

Online Supplementary Materials

Supplementary data associated with this article can be found in the online version at doi: 10.1016/j.mencom.2018.03.019.

References

1 T. T. Thuy, S. Maenosono and N. T. K. Thanh, in *Magnetic Nanoparticles. From Fabrication to Clinical Applications: Theory to Therapy, Chemistry to Clinic, Bench to Bedside*, ed. N. T. K. Thanh, CRC Press, London, 2012, p. 99.

2 C. Sun, J. S. H. Lee and M. Zhang, *Adv. Drug Deliv. Rev*., 2008, **60**, 1252.

3 V. Nadwana, M. De, S. Chu, M. Jaiswal, M. Rotz, T. J. Meade and V. P. Dravid, in *Nanotechnology-Based Precision Tools for the Detection and Treatment of Cancer*, eds. C. Mirkin, Th. J. Meade, S. H. Petrosko and A. H. Stegh, Springer, 2015, pp. 51–83.

4 C. R. De Silva, S. Smith, I. Shim, J. Pyun, T. Gutu, J. Jiao and Z. Zheng, *J. Am. Chem. Soc*., 2009, **131**, 6336.

5 (*a*) D. Ling, N. Lee and T. Hyeon, *Acc. Chem. Res*., 2015, **48**, 1276; (*b*) V. M. Shkinev, Yu. A. Zakhodyaeva, R. Kh. Dzhenloda, O. B. Mokhodoeva and A. A. Voshkin, *Mendeleev Commun*., 2017, **27**, 485; (*c*) I. N. Topchieva, V. V. Spiridonov, A. N. Zakharov, M. I. Afanasov, A. V. Mironov, N. S. Perov and A. S. Semisalova, *Mendeleev Commun*., 2015, **25**, 145.

6 H. Cui, D. Li and Z. Zhang, *Mater. Lett*., 2015, **143**, 38.

7 M. Baghbanzadeh, L. Carbone, P. D. Cazzoli and C. O. Kappe, *Angew. Chem. Int. Ed*., 2011, **50**, 11312.

8 (*a*) T. A. Lastovina, V. E. Guterman and S. S. Manokhin, *Al'ternativnaya Energetika i Ecologiya (ISJAEE)*, 2011, no. 9, 111 (in Russian); (*b*) A. Mezni, I. Balti, A. Mlayah, N. Jouini and L. S. Smiri, *J. Phys. Chem. C*, 2013, **117**, 16166; (*c*) K. C.-F. Leung, S. Xuan, X. Zhu, D. Wang, C.-P. Chak, S.-F. Lee, W. K.-W. Ho and B. C.-T. Chung, *Chem. Soc. Rev*., 2012, **41**, 1911.

9 (*a*) T. A. Lastovina, A. L. Bugaev, S. P. Kubrin, E. A. Kudryavtsev and A. V. Soldatov, *J. Struct. Chem*., 2016, **57**, 1444 (*Zh. Strukt. Khim*., 2016, **57**, 1523); (*b*) T. A. Lastovina, A. P. Budnyk, E. A. Kudryavtsev, A. V. Nikolsky, A. T. Kozakov, N. K. Chumakov, A. V. Emelyanov and A. V. Soldatov, *Mater. Sci. Eng. C*, 2017, **80**, 110; (*c*) T. A. Lastovina, A. P. Budnyk, M. A. Soldatov, Yu. V. Rusalev, A. A. Guda, A. S. Bogdan and A. V. Soldatov, *Mendeleev Commun*., 2017, **27**, 487.

10 W. Baaziz, B. P. Pichon, S. Fleutot, Y. Liu, C. Lefevre, J.-M. Greneche, M. Toumi, T. Mhiri and S. Begin-Colin, *J. Phys. Chem. C*, 2014, **118**, 3795.

11 W. Huan, C. Cheng, Y. Yang, H. Yuan and Y. Li, *J. Nanosci. Nanotechnol*., 2012, **12**, 4621.

12 (*a*) R. E. Vandenberghe and E. De Grave, in *Mössbauer Spectroscopy – Tutorial Book*, eds. Y. Yoshida and G. Langouche, Springer, Berlin, 2013, p. 91; (*b*) F. Menil, *J. Phys. Chem. Solids*, 1985, **46**, 763.

13 P. G. Rudakovskaya, E. K. Beloglazkina, A. G. Majouga and N. V. Zyk, *Mendeleev Commun*., 2010, **20**, 158.

14 B. Ankamwar, T. C. Lai, J. H. Huang, R. S. Liu, M. Hsiao, C. H. Chen and Y. K. Hwu, *Nanotechnology*, 2010, **21**, 075102.

Received: 30th August 2017; Com. 17/5343